Rhenium(I) Terpyridine π-Bases: Reversible η²-Coordination of Ketones, Aldehydes, and Olefins in the Terpyridine Plane

Lisa E. Helberg, T. Brent Gunnoe, Benjamin C. Brooks, Michal Sabat, and W. Dean Harman*

Department of Chemistry, The University of Virginia, Charlottesville, Virginia 22901

Received June 17, 1998

The complex *trans*-[Re(terpy)(Br)(PPh_3)$_2$][OTf] (**2**) (terpy = 2,2′:6′,2″-terpyridine) is a convenient precursor to the electron-rich π-basic fragment {(terpy)(L)$_2$Re}$^+$ (L = ^{t}BuNC or PMe_3). Reduction of **2** with activated magnesium in the presence of unsaturated organic molecules and an excess of either ^{t}BuNC or PMe_3 yields complexes of the type *trans*-[(terpy)(L)$_2$Re(η²-π)][OTf] (L = ^{t}BuNC or PMe_3; π = olefin, aldehyde, or ketone). The dihaptocoordinated organic moieties show a preference for binding in the plane of the terpy ligand. Reaction of *trans*-[Re(terpy)(^{t}BuNC)$_2$(η²-acetone)][OTf] (**9**) with MeOTf yields an observable η²-ketonium complex. The electronic environment of these complexes has been probed by cyclic voltammetry, and the details of ligand exchange for the η²-ketone complexes are presented. Geometric features determined from X-ray crystal structure analyses of *trans*-[(terpy)(^{t}BuNC)$_2$Re(η²-cyclopentene)][OTf] (**4**) and *trans*-[(terpy)(^{t}BuNC)$_2$Re(η²-acetophenone)][OTf] (**11**) are reported.

Introduction

Aldehydes and ketones have played an important role in the field of organic chemistry, and much is known about the reactivity of these carbonyl compounds.[1] One of the great utilities of transition metal chemistry is the ability to enhance the reactivity of organic compounds upon binding them to a metal fragment.[2] Although metal-bound carbonyl compounds were known prior to 1970,[3] research in this field has gained intensity only recently. A large variety of aldehyde and ketone complexes have been isolated and characterized, and the reactivity of metal-bound carbonyl compounds has been described.[4−10]

Two bonding modes exist for aldehyde and ketone complexes: η¹ (σ-complex) bound through oxygen and η² (π-complex) bound through both carbon and oxygen (Scheme 1).[11] Gladysz et al. have performed an elegant series of studies concerning the relative reactivity and equilibria of σ/π-bonding modes for aldehyde and ketone complexes of rhenium,[6i,8i] and the η¹ to η² interconversion has been studied in detail for [$(NH_3)_5$Ru(acetone)]$^{3+/2+}$ [9f] and [$(NH_3)_5$Os(acetone)]$^{3+/2+}$.[9h] The effect of the metal center on σ/π-bonding modes for group VI aldehyde complexes has also been probed.[6l]

Scheme 1. η¹ and η² Bonding Modes for Aldehydes and Ketones

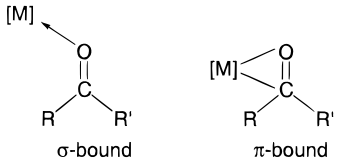

Whereas a number of aldehyde complexes have been reported, and both coordination modes are common,[5,6] well-characterized examples of η²-ketone complexes are rare. Several π-coordinated ketone complexes have been observed;[8−10] however, the majority of these ketones possess electron-withdrawing substituents.[8] Systematic studies of η²-ketone complexes bearing simple alkyl substituents are uncommon.[9a−e] The scarcity of η²-ketone complexes compared to their aldehyde analogues has been attributed to both electronic and steric factors. The π* orbital that participates in metal-to-ligand backbonding lies higher in energy for ketones compared to the π* orbital of aldehydes, and the disubstituted carbonyl of ketones is more sterically imposing than the singly substituted carbonyl of aldehydes.[4a]

We recently reported a synthesis of unusually electron-rich Re^I coordination complexes from the reduction of *trans*-[Re(terpy)(Cl)(PPh_3)$_2$]$^+$ (terpy = 2,2′:6′,2″-terpyridine).[12] Although this material served as a useful precursor to activated olefin complexes of rhenium(I), reduction of *trans*-[Re(terpy)(Cl)(PPh_3)$_2$]$^+$ in the presence of other unsaturated ligands (e.g., aldehydes, ketones, and arenes) produced only intractable mixtures of products. Hoping that replacement of the chloride

(1) Smith, M. B. *Organic Synthesis*; McGraw-Hill: New York, 1994.
(2) (a) Hegedus, L. E. *Transition Metals in the Synthesis of Complex Organic Molecules*; University Science Books: Mill Valley, CA, 1994. (b) Crabtree, R. H. *The Organic Chemistry of the Transition Metals*; Wiley-Interscience: New York, 1994. (c) Collman, J. P.; Hegedus, L. S.; Norton, J. R.; Finke, R. G. *Principles and Applications of Organotransition Metal Chemistry*; University Science Books: Mill Valley, CA, 1987.
(3) See, for example: Clarke, B.; Green, M.; Osborn, R. B. L.; Stone, F. G. A. *J. Chem. Soc. A* **1968**, 167.
(4) For reviews of transition metal aldehyde and ketone complexes, see: (a) Huang, Y.-H.; Gladysz, J. A. *J. Chem. Educ.* **1988**, *65*, 298. (b) Shambayati, S.; Schreiber, S. L. In *Comprehensive Organic Synthesis*; Trost, B. M., Fleming, I., Schreiber, S. L., Eds.; Pergamon: New York, 1991; Vol. 1, Chapter 1.10.

10.1021/om980500p CCC: $18.00
Publication on Web 01/22/1999

ligand by a better leaving group would enhance the utility of this approach, we prepared the complex *trans*-[Re(terpy)(Br)(PPh_3)$_2$][OTf] (**2**). Unlike its chloride predecessor, this material has proven to be a versatile precursor to Re^{I} terpy complexes of the form *trans*-[(terpy)(L)$_2$Re(η^2-π)]$^+$ (where L = PMe_3, ^{t}BuNC; π = cyclopentene, benzaldehyde, acetone, and acetophenone). The coordination details, electrochemistry, solid-state geometrical features, and reactivity for this set of complexes are reported below.

Scheme 2. Synthesis of *trans*-[Re(terpy)L$_2$(π)]$^+$ (where π = Olefin, Ketone, or Aldehyde)

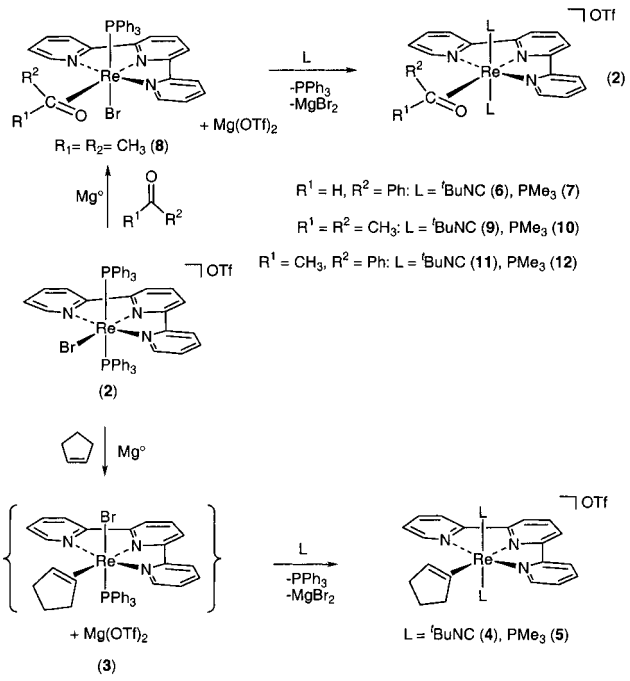

Results

Reaction of the chelate complex (Br)$_2$(PPh_3)$_2$Re(=N−N=C(Ph)−O−) (**1**) with excess terpy in a benzene/MeOH (1:1 v/v) mixture, followed by counterion metathesis upon treatment with AgOTf, produces *trans*-[Re(terpy)(Br)(PPh_3)$_2$][OTf] (**2**). Complex **2** is characterized by combustion analysis and electrochemistry, as compared with the previously reported complex *trans*-[Re(terpy)(Cl)(PPh_3)$_2$][OTf].[12]

Reaction with Cyclopentene. Reduction of **2** in the presence of cyclopentene yields a new compound assigned as (terpy)Re(Br)(PPh_3)(η^2-cyclopentene) (**3**) (Scheme 2). Complex **3** is not isolable but can be observed by cyclic voltammetry. The positive shift in the

(5) For examples of η^2-formaldehyde complexes, see: (a) Brown, K. L.; Clark, G. R.; Headford, C. E. L.; Marsden, K.; Roper, W. R. *J. Am. Chem. Soc.* **1979**, *101*, 503. (b) Clark, G. R.; Headford, C. E. L.; Marsden, K.; Roper, W. R. *J. Organomet. Chem.* **1982**, *231*, 335. (c) Headford, C. E. L.; Roper, W. R. *J. Organomet. Chem.* **1983**, *244*, C53. (d) Berke, H.; Huttner, G.; Weiler, G.; Zsolnai, L. *J. Organomet. Chem.* **1981**, *219*, 353. (e) Gambarotta, S.; Floriani, C.; Chiesi-Villa, A.; Guastini, C. *J. Am. Chem. Soc.* **1982**, *104*, 2019. (f) Gambarotta, S.; Floriani, C.; Chiesi-Villa, A.; Guastini, C. *J. Am. Chem. Soc.* **1985**, *107*, 2985. (g) Gambarotta, S.; Floriani, C.; Chiesi-Villa, A.; Guastini, C. *Organometallics* **1986**, *5*, 2425. (h) Head, R. A. *J. Chem. Soc., Dalton Trans.* **1982**, 1637. (i) Buhro, W. E.; Patton, A. T.; Strouse, C. E.; Gladysz, J. A.; McCormick, F. B.; Etter, M. C. *J. Am. Chem. Soc.* **1983**, *105*, 1056. (j) Green, M. L. H.; Parkin, G.; Moynihan, K. J.; Prout, K. *J. Chem. Soc., Chem. Commun.* **1984**, 1540. (k) Green, M. L. H.; Parkin, G. *J. Chem. Soc., Chem. Commun.* **1986**, 90. (l) Herberich, G. E.; Okuda, J. *Angew. Chem., Int. Ed. Engl.* **1985**, *24*, 402. (m) LaPointe, R. E.; Wolczanski, P. T. *J. Am. Chem. Soc.* **1986**, *108*, 3535. (n) LaPointe, R. E.; Wolczanski, P. T.; Mitchell, J. F. *J. Am. Chem. Soc.* **1986**, *108*, 6382. (o) Assett, A.; Burger, B. J.; Gibson, V. C.; Bercaw, J. E. *J. Am. Chem. Soc.* **1986**, *108*, 5347.

(6) For examples of transition metal aldehyde complexes, see: (a) Brunner, H.; Wachter, J.; Bernal, I.; Creswick, M. *Angew. Chem., Int. Ed. Engl.* **1979**, *18*, 861. (b) Gauntlett, J. T.; Taylor, B. F.; Winter, M. J. *J. Chem. Soc., Chem. Commun.* **1984**, 420. (c) Gauntlett, J. T.; Taylor, B. F.; Winter, M. J. *J. Chem. Soc., Dalton Trans.* **1985**, 1815. (d) Jones, C. J.; McCleverty, J. A.; Rothin, A. S. *J. Chem. Soc., Dalton Trans.* **1986**, 2109. (e) Poddar, R. K.; Sarma, K. P.; Sarma, U. C. *Polyhedron* **1985**, *4*, 1419. (f) Walther, D. *J. Organomet. Chem.* **1980**, *190*, 393. (g) Fernández, J. M.; Emerson, K.; Carsen, R. H.; Gladysz, J. A. *J. Am. Chem. Soc.* **1986**, *108*, 8268. (h) Garner, C. M.; Méndez, N. Q.; Kowalczyk, J. J.; Fernández, J. M.; Emerson, K.; Larsen, R. D.; Gladysz, J. A. *J. Am. Chem. Soc.* **1990**, *112*, 5146. (i) Méndez, N. Q.; Seyler, J. W.; Arif, A. M.; Gladysz, J. A. *J. Am. Chem. Soc.* **1993**, *115*, 2323. (j) Boone, B. J.; Klein, D. P.; Seyler, J. W.; Méndez, N. Q.; Arif, A. M.; Gladysz, J. A. *J. Am. Chem. Soc.* **1996**, *118*, 2411. (k) Wang, Y.; Agbossou, F.; Dalton, D. M.; Liu, Y.; Arif, A. M.; Gladysz, J. A. *Organometallics* **1993**, *12*, 2699. (l) Schuster, D. M.; White, P. S.; Templeton, J. L. *Organometallics* **1996**, *15*, 5467. (m) Rabinovich, D.; Parkin, G. *J. Am. Chem. Soc.* **1991**, *113*, 5904. (n) Adams, H.; Bailey, N. A.; Gauntlett, J. T.; Winter, M. J.; Woodward, S. *J. Chem. Soc., Dalton Trans.* **1991**, 2217. (o) Denmark, S. E.; Almstead, N. G. *J. Am. Chem. Soc.* **1993**, *115*, 3133. (p) Faller, J. W.; Ma, Y. *J. Am. Chem. Soc.* **1991**, *113*, 1579. (q) Bullock, R. M.; Rappoli, B. J. *J. Am. Chem. Soc.* **1991**, *113*, 1659. (r) Cicero, R. L.; Protasiewicz, J. D. *Organometallics* **1995**, *14*, 4792. (s) Faller, J. W.; Ma, Y.; Smart, C. J.; DiVerdi, M. J. *J. Organomet. Chem.* **1991**, *420*, 237. (t) Caldarelli, J. L.; Wagner, L. E.; White, P. S.; Templeton, J. L. *J. Am. Chem. Soc.* **1994**, *116*, 2878. (u) Bonnesen, P. V.; Puckett, C. L.; Honeychuck, R. V.; Hersh, W. H. *J. Am. Chem. Soc.* **1989**, *111*, 6070.

(7) For examples of η^1-ketone complexes, see: (a) Foxman, B. M.; Klemarczyk, P. T.; Liptrot, R. E.; Rosenblum, M. *J. Organomet. Chem.* **1980**, *187*, 253. (b) Boudjouk, P.; Woell, J. B.; Radonovich, L. J.; Eyring, M. W. *Organometallics* **1982**, *1*, 582. (c) Crabtree, R. H.; Hlatky, G. G.; Parnell, C. P.; Segmüller, B. E.; Uriarte, R. J. *Inorg. Chem.* **1984**, *23*, 354. (d) Courtot, P.; Pichon, R.; Salaün, J. Y. *J. Organomet. Chem.* **1985**, *286*, C17. (e) Auffret, J.; Courtot, P.; Pichon, R.; Salaün, J. Y. *J. Chem. Soc., Dalton Trans.* **1987**, 1687. (f) Dalton, D. M.; Fernández, J. M.; Emerson, K.; Larsen, R. D.; Arif, A. M.; Gladysz, J. A. *J. Am. Chem. Soc.* **1990**, *112*, 9198. (g) Dalton, D. M.; Gladysz, J. A. *J. Chem. Soc., Dalton Trans.* **1991**, 2741. (h) Sünkel, K.; Urban, G.; Beck, W. *J. Organomet. Chem.* **1985**, *290*, 231. (i) Bachand, B.; Wuest, J. D. *Organometallics* **1991**, *10*, 2015. (j) Gambarotta, S.; Pasquali, M.; Floriani, C.; Chiesi-Villa, A.; Guastini, C. *Inorg. Chem.* **1981**, *20*, 1173. (k) See also refs 5m, 5r, 5u, and 5v.

(8) For examples of η^2-ketones with halogen-containing electron-withdrawing groups, see: (a) Clemens, J.; Green, M.; Stone, F. G. A. *J. Chem. Soc., Dalton Trans.* **1973**, 375. (b) Countryman, R.; Penfold, B. R. *J. Chem. Soc., Chem. Commun.* **1971**, 1598. (c) Ittel, S. D. *J. Organomet. Chem.* **1977**, *137*, 223. (d) Ittel, S. D. *Inorg. Chem.* **1977**, *16*, 2589. (e) Green, M.; Howard, J. A. K.; Laguna, A.; Smart, L. E.; Spencer, J. L.; Stone, F. G. A. *J. Chem. Soc., Dalton Trans.* **1977**, 278. (f) Burgess, J.; Chambers, J. G.; Clarke, D. A.; Kemmitt, R. D. W. *J. Chem. Soc., Dalton Trans.* **1977**, 1906. (g) Clarke, D. A.; Hunt, M. M.; Kemmitt, R. D. W. *J. Organomet. Chem.* **1979**, *175*, 303. (h) Grassi, A.; Longo, P.; Musco, A.; Porzio, W.; Scrivanti, A. *J. Organomet. Chem.* **1985**, *289*, 439. (i) Klein, D. P.; Dalton, D. M.; Méndez, N. Q.; Arif, A. M.; Gladysz, J. A. *J. Organomet. Chem.* **1991**, *412*, C7.

(9) For examples of η^2-ketones with alkyl or aryl substituents, see: (a) Williams, D. S.; Schofield, M. H.; Anhaus, J. T.; Schrock, R. R. *J. Am. Chem. Soc.* **1990**, *112*, 6728. (b) Barry, J. T.; Chacon, S. T.; Chisholm, M. H.; Huffmann, J. C.; Streib, W. E. *J. Am. Chem. Soc.* **1995**, *117*, 1974. (c) Harman, W. D.; Fairlie, D. P.; Taube, H. *J. Am. Chem. Soc.* **1986**, *108*, 8223. (d) Burkey, D. J.; Debad, J. D.; Legzdins, P. *J. Am. Chem. Soc.* **1997**, *119*, 1139. (e) Bryan, J. C.; Mayer, J. M. *J. Am. Chem. Soc.* **1990**, *112*, 2298. (f) Powell, D. W.; Lay, P. A. *Inorg. Chem.* **1992**, *31*, 3542. (g) Tsou, T. T.; Huffman, J. C.; Kochi, J. K. *Inorg. Chem.* **1979**, *18*, 2311. (h) Harman, W. D.; Sekine, M.; Taube, H. *J. Am. Chem. Soc.* **1988**, *110*, 2439. (i) Harman, W. D.; Dobson, J. C.; Taube, H. *J. Am. Chem. Soc.* **1989**, *111*, 3061. (j) Hill, J. E.; Fanwick, P. E.; Rothwell, I. P. *Organometallics* **1992**, *11*, 1771. (k) Okuda, J.; Herberich, G. E. *Organometallics* **1987**, *6*, 2331. (l) Chisholm, M. H.; Folting, K.; Klang, J. A. *Organometallics* **1990**, *9*, 607.

(10) For examples of η^2-ketones (with alkyl or aryl substituents) formed from carbonylation reactions, see: (a) Erker, G.; Dorf, U.; Czisch, P.; Petersen, J. L. *Organometallics* **1986**, *5*, 668. (b) Wood, C. D.; Schrock, R. R. *J. Am. Chem. Soc.* **1979**, *101*, 5421. (c) Mayer, J. M.; Bercaw, J. E. *J. Am. Chem. Soc.* **1982**, *104*, 2157.

(11) Within the context of η^2 bonding, some bound η^2-ketones can be described as metalloxiranes. For a theoretical discussion of η^2 versus η^1 bonding, see: Delbecq, F.; Sautet, P. *J. Am. Chem. Soc.* **1992**, *114*, 2446.

(12) Helberg, L. E.; Barrera, J.; Sabat, M.; Harman, W. D. *Inorg. Chem.* **1995**, *34*, 2033.

Scheme 3. NOE Measurements in Support of the Assigned Dominant Solution Rotomer of 4

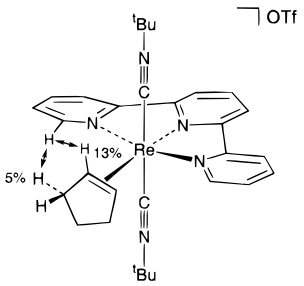

Re^{II}/Re^{I} reduction potential for this complex ($E_{p,a} = 0.1$ V vs NHE) compared to that of **2** is consistent with replacement of a phosphine in the coordination set of **2** with the olefin. In situ reaction of **3** with excess ^{t}BuNC or PMe_3 yields *trans*-[(terpy)$(L)_2$Re(η^2-cyclopentene)]-[OTf] [L = ^{t}BuNC (**4**); PMe_3 (**5**)] (Scheme 2).

Proton and carbon NMR and electrochemical data, as well as a solid-state X-ray structural study of **4** (vide infra), confirm the identities of **4** and **5**. Upfield chemical shifts for the bound olefinic protons (3.8−4.7 ppm) in the ^{1}H NMR spectrum and ^{13}C NMR resonances for the bound carbon atoms (64−66 ppm) are consistent with an η^2-bound olefin. The inequivalence of the ^{t}BuNC and PMe_3 ligands in **4** and **5**, respectively, is consistent with either trans or cis geometries. ^{1}H NMR NOE experiments suggest that the cyclopentene ligand is bound in the plane of the terpy moiety with a trans configuration for the isonitrile or phosphine ligands. For complex **4**, a large NOE interaction is observed between the ortho proton on the terpy ligand and the olefinic protons (13%) as well as an enhancement (5%) between the same terpy proton and one of the diastereotopic cyclopentene protons (Scheme 3). Both interactions are concordant with the geometry of **4** in the solid state (vide infra), and similar enhancements (12 and 9%) are observed for the PMe_3 complex **5**.

Reaction with Benzaldehyde. Analogous to the reaction of *trans*-[Re(terpy)(Br)$(PPh_3)_2$][OTf] (**2**) with cyclopentene, the reduction of **2** with Zn/Hg in the presence of benzaldehyde produces a new product that exhibits a cyclic voltammogram consistent with the formation of (terpy)Re(Br)(PPh_3)(η^2-benzaldehyde). Again, isolation of a new product was only possible after in situ addition of ^{t}BuNC or PMe_3. Isolation of *trans*-[(terpy)-$(L)_2$Re(η^2-benzaldehyde)][OTf] {L = ^{t}BuNC (**6**); PMe_3 (**7**)} was achieved in 80 and 93% yield, respectively (Scheme 2). Upfield chemical shifts for the aldehydic proton and the carbonyl carbon in the ^{1}H and ^{13}C NMR spectra are diagnostic for dihapto-coordinated aldehyde ligands.[4a] Resonances at 6.65 and 6.75 ppm (^{1}H NMR spectrum) are assigned to the aldehyde protons of **6** and **7**, respectively, and the ^{13}C NMR spectra show upfield chemical shifts for the carbonyl carbons (**6**, 86.1 ppm; **7**, 83.6 ppm).

Reactions with Ketones. The ability of the electron-rich *trans*-{(terpy)$(L)_2$Re}$^+$ fragment to bind olefins and benzaldehyde in an η^2 fashion prompted our exploration into the coordination of ketones. Specifically, we sought to probe the π-basicity of the rhenium metal center by comparing the proclivity for π versus σ binding of alkyl and aryl ketones.

Magnesium reduction of **2** in neat acetone yields (terpy)(Br)(PPh_3)Re(η^2-acetone) (**8**; Scheme 2). Rotation of the ketone is hindered on the time scale of the NMR experiment as indicated by two resonances in the ^{1}H NMR spectrum for the methyl substituents of the acetone ligand. While sterics may contribute to this hindered rotation, it is likely that the dπ orbital discrepancy caused by back-bonding with the terpy and phosphine ligands contributes significantly to the rotational barrier. The ketone ligand of **8** is labile. An acetone-d_6 solution of **8** slowly exchanges the protioacetone ligand with the deuterated solvent. Thus, over time the resonances for the bound ligand disappear, and incipient resonances for free acetone are observed. Resonances for partially deuterated species due to proton exchange were not observed.

In situ reaction of **8** with ^{t}BuNC or PMe_3 results in the displacement of PPh_3 and bromide (Scheme 2). In neither case is the displacement of acetone observed. Spectral features for *trans*-[(terpy)(^{t}BuNC)$_2$Re(η^2-acetone)][OTf] (**9**) and *trans*-[(terpy)$(PMe_3)_2$Re(η^2-acetone)]-[OTf] (**10**) are similar to those of **8**. The ^{13}C NMR spectra for **9** and **10** indicate resonances for the bound carbonyl carbons at 89.6 and 88.7 ppm, respectively. A notable difference from complex **8** is the equivalence of the methyl groups of the acetone ligand in the ^{1}H NMR spectra of **9** and **10**. This equivalence is consistent with coordination of acetone in the plane of the terpy ligand. NOE enhancements are observed between the methyl resonances of the ketone and one of the terpy protons (21% for **9**; 16% for **10**). For complex **10**, interactions are noted between the methyl groups of the PMe_3 ligand and the acetone ligand (5%) and between the phosphine ligands and terpy protons (4%).

The dihapto-coordinated acetophenone complexes *trans*-[(terpy)$(L)_2$Re(η^2-π)](OTf) (L = ^{t}BuNC or PMe_3; π = acetophenone (**11**, **12**)) can be prepared by reaction sequences similar to the preparation of **9** and **10** (Scheme 2). The (terpy)(Br)(PPh_3)Re(η^2-acetophenone) intermediate can be observed with electrochemical experiments; however, unlike complex **8,** this putative complex eluded isolation. The *trans*-{(terpy)$(L)_2$Re}$^+$ fragments have also been observed spectroscopically (^{1}H NMR) to form stable complexes with benzophenone and 2-butanone, although detailed characterization of these complexes was frustrated by the presence of impurities.

The observation of (terpy)Re(Br)(PPh_3)(η^2-cyclopentene) (**3**) and (terpy)Re(Br)(PPh_3)(η^2-acetone) (**8**) and their facile conversion to *trans*-[(terpy)$(L)_2$Re(π)][OTf] (π = cyclopentene or acetone; L = ^{t}BuNC, **4**, **9**; L = PMe_3, **5**, **10**) provides direct evidence for the mechanism of formation of the dihapto-coordinated complexes (Scheme 4). A single electron reduction of *trans*-[Re-(terpy)(Br)$(PPh_3)_2$][OTf] (**2**) with Mg results in the loss of a single phosphine ligand and coordination of the unsaturated organic ligand (π) to yield (terpy)Re(Br)-(PPh_3)(η^2-π). It is difficult to discern between initial loss of bromide followed by coordination of π and displacement of a phosphine ligand by bromide (path A) and the other possible route, simple loss of phosphine, rearrangement, and coordination of π (path B). In situ reaction of (terpy)Re(Br)(PPh_3)(π) with excess ^{t}BuNC or PMe_3 yields *trans*-[(terpy)$(L)_2$Re(η^2-π)][OTf] (L = ^{t}BuNC, PMe_3). The nature of the halide ligand seemingly plays

Scheme 4. Possible Mechanisms for the Replacement of PPh_3 by π (where π = Olefin, Ketone, or Aldehyde; L = PMe_3, ^{t}BuNC)

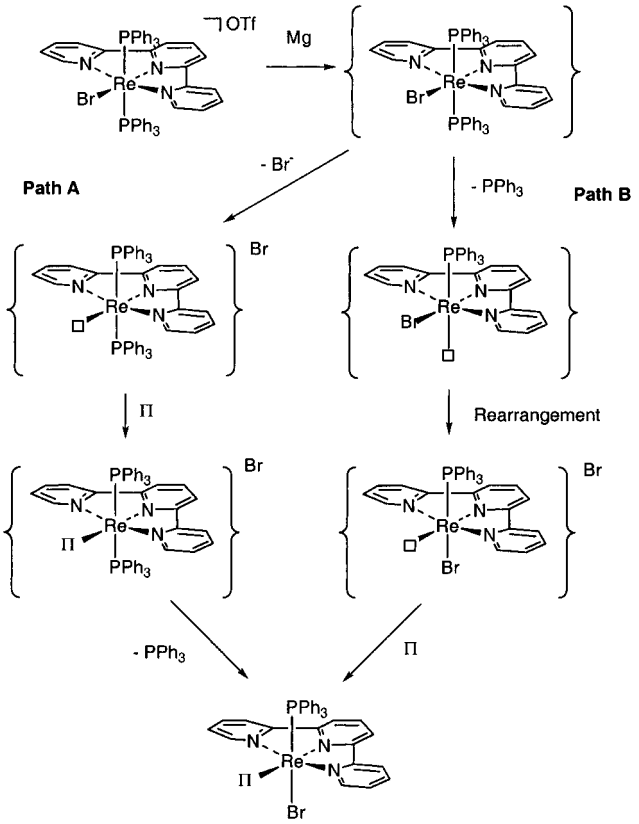

a vital role in these reactions. If bromide is replaced with chloride, access to *trans*-[(terpy)$(L)_2$Re(η^2-π)][OTf] complexes is lost.[12]

Solid-State Structural Studies. Single-crystal X-ray diffraction studies have provided geometric details of the solid-state structures of *trans*-[(terpy)(^{t}BuNC)$_2$Re-(η^2-cyclopentene)][OTf] (**4**) and *trans*-[(terpy)(^{t}BuNC)$_2$Re-(η^2-acetophenone)][OTf] (**11**). ORTEP diagrams for **4** and **11** are depicted in Figures 1 and 2, and relevant crystallographic data and collection parameters and selected bond lengths and angles are presented in Tables 1 and 2.

The structure of **4** is consistent with the assigned stereochemistry (vide supra), including coordination of cyclopentene in the plane of the terpy ligand with trans ^{t}BuNC ligands (Figure 1). The olefinic C−C bond length of 1.46 Å is elongated from that of unbound cyclopentene (1.39 Å). The increase in bond length is indicative of metal back-bonding into the π^* orbital of the olefinic ligand. The cyclopentene ligand is complexed in an approximately symmetrical fashion. The rhenium−carbon bond distances of 2.21 and 2.22 Å are typical of rhenium−olefin complexes.[13] The bond distances from rhenium to the terpy nitrogen atoms cis to cyclopentene are longer than the coordinated nitrogen juxtaposed trans to the olefin ligand (2.166(9) and 2.148(9) Å vs 2.04(1) Å).

The structure of **11** confirms the designated π bonding of the ketone ligand (Figure 2). The C−O bond length

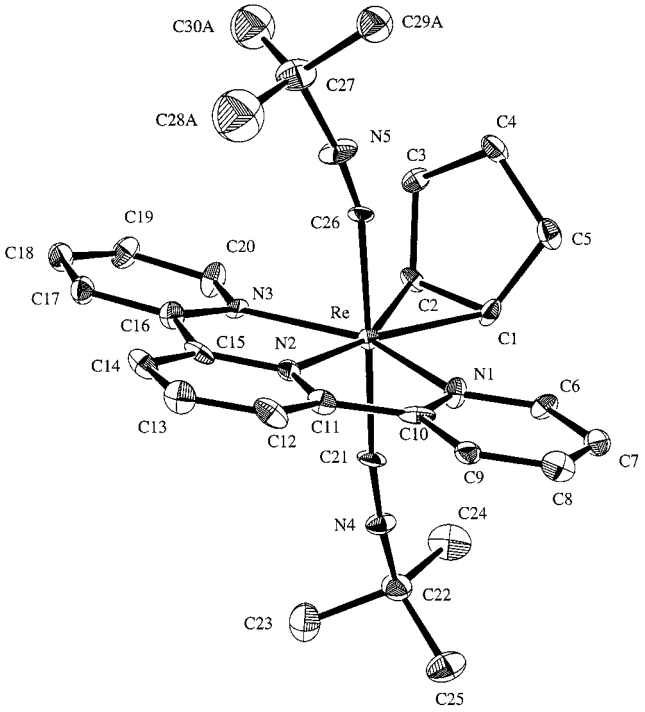

Figure 1. ORTEP diagram for the complex *trans*-[Re-(terpy)(^{t}BuNC)$_2$(η^2-cyclopentene)][OTf] (**4**).

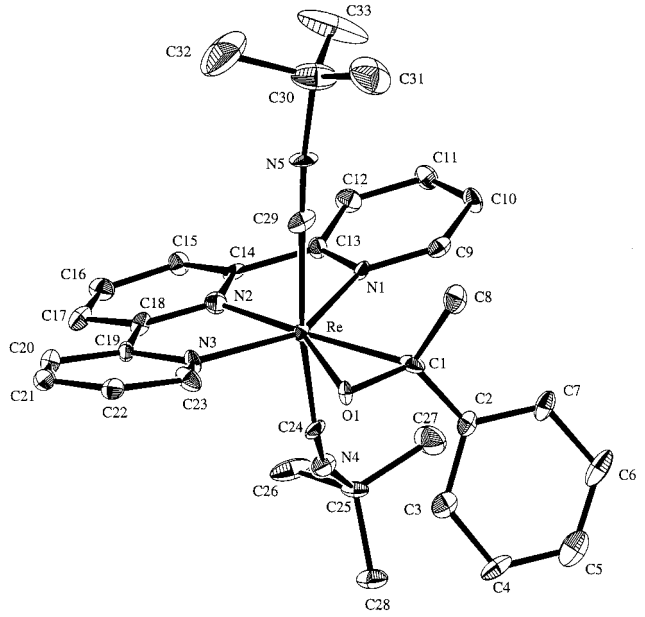

Figure 2. ORTEP diagram for the complex *trans*-[Re-(terpy)(^{t}BuNC)$_2$(η^2-acetophenone)][OTf] (**11**).

of 1.37 Å is increased from unbound acetophenone (1.26 Å).[14] As with complex **4**, the coordination of the unsaturated organic molecule occurs in the plane of the terpy ligand, leaving the isonitrile ligands in a trans configuration. The Re−C(1) bond length is 2.17 Å, while the Re−O_1 distance is 2.02 Å. Direct comparison of the structural features of **11** with other rhenium−ketone complexes is difficult due to a lack of such examples. However, the rhenium−carbon and rhenium−oxygen bond lengths are similar to those reported for a series of rhenium η^2-aldehyde complexes.[6j] As is observed with

(13) See, for example: (a) Bodner, G. S.; Fernández, J. M.; Arif, A. M.; Gladysz, J. A. *J. Am. Chem. Soc.* **1988**, *110*, 4082. (b) Bodner, G. S.; Peng, T.; Arif, A. M.; Gladysz, J. A. *Organometallics* **1990**, *9*, 1191.

(14) The C−O bond length is similar to other reported distances for η^2-ketones. See, for example, refs 9b, 9c, 9e, 9j, and 9l.

Table 1. Selected Crystallographic Data for [Re(terpy)(ᵗBuNC)$_2$(η^2-cyclopentene)][OTf] (4) and [Re(terpy)(ᵗBuNC)$_2$(η^2-acetophenone)][OTf] (11)

	[Re(terpy)(ᵗBuNC)$_2$ (η^2-cyclopentene)] [OTf]·Et$_2$O (**4**)	[Re(terpy)(ᵗBuNC)$_2$ (η^2-acetophenone)] [OTf] (**11**)
formula	$C_{35}H_{47}N_5F_3O_4SRe$	$C_{34}H_{37}N_5F_3O_4SRe$
mol wt	877.05	854.96
cryst syst	monoclinic	triclinic
space group	$P2_1/n$ (No. 14)	$P\bar{1}$ (No. 2)
a, Å	14.266(3)	11.534(5)
b, Å	15.801(5)	16.597(7)
c, Å	17.482(5)	9.805(4)
α, deg	90	103.03(3)
β, deg	107.76(2)	94.90(3)
γ, deg	90	103.13(3)
V, Å^3	3758(3)	1762(3)
Z	4	2
D_{calcd}, g cm^{-3}	1.55	1.61
cryst dimens, mm	0.38 × 0.32 × 0.11	0.32 × 0.23 × 0.46 mm
temp, °C	−120	−120
radiation (λ, Å)	0.710 69	0.710 69
2θ max, deg	46	46
μ(Mo Kα), cm^{-1}	33.85	36.08
R	0.047	0.056
R_w	0.060	0.072

Table 2. Selected Bond Distances and Angles for [Re(terpy)(ᵗBuNC)$_2$(η^2-cyclopentene)][OTf] (4) and [Re(terpy)(ᵗBuNC)$_2$(η^2-acetophenone)][OTf] (11)

4		**11**	
	Bond Distances (Å)		
Re−C1	2.22(1)	Re−C1	2.17(1)
Re−C2	2.21(1)	Re−O1	2.024(7)
Re−N1	2.166(9)	Re−N1	2.13(1)
Re−N2	2.04(1)	Re−N2	2.03(1)
Re−N3	2.148(9)	Re−N3	2.152(9)
Re−C21	2.06(1)	Re−C24	2.09(1)
Re−C26	2.05(1)	Re−C29	2.09(1)
C1−C2	1.46(2)	C1−O1	1.37(1)
	Bond Angles (deg)		
C1−Re−C21	83.4(5)	C1−Re−C24	90.3(4)
C2−Re−C21	85.5(5)	O1−Re−C24	93.6(4)
C1−Re−C26	95.6(5)	C1−Re−C29	89.9(4)
C2−Re−C26	90.7(4)	O1−Re−C29	94.5(4)
C1−Re−N1	86.3(4)	C1−Re−N1	92.0(4)
C2−Re−N1	124.9(4)	C1−Re−N2	165.6(4)
C1−Re−N2	160.0(4)	C1−Re−N3	117.9(4)
C2−Re−N2	160.3(4)	O1−Re−N1	129.8(3)
C1−Re−N3	123.9(4)	O1−Re−N2	154.0(4)
C2−Re−N3	85.4(4)	O1−Re−N3	80.3(3)
N1−Re−N3	149.7(4)	N1−Re−N3	149.6(3)
N1−Re−N2	74.1(4)	N1−Re−N2	75.2(4)
N2−Re−N3	75.7(4)	N2−Re−N3	75.7(4)
N1−Re−C21	90.3(4)	N1−Re−C24	82.8(4)
N1−Re−C26	94.6(4)	N1−Re−C29	84.3(4)
N2−Re−C21	100.6(5)	N2−Re−C24	81.7(4)
N2−Re−C26	82.0(4)	N2−Re−C29	95.2(4)
N3−Re−C21	92.5(4)	N3−Re−C24	101.8(4)
N3−Re−C26	84.0(4)	N3−Re−C29	89.5(5)
Re−C1−C5	120.8(8)	Re−C1−C8	118.5(8)
Re−C2−C3	119.2(8)	Re−C1−C2	121.4(8)

the cyclopentene complex **4**, the rhenium−nitrogen bond distance trans to the unsaturated organic ligand is shorter than the distance to the cis nitrogen atoms (2.13(1) and 2.152(9) Å vs 2.03(1) Å).

Although it is sterically the least favorable position, coordination in the plane of the terpy ligand is observed for all of the dihapto-coordinated complexes. The fact that the unsaturated organic compounds bind in this sterically hindered position reflects a strong electronic

Scheme 5. Molecular Orbital Diagram for Complexes of the Form [Re(terpy)(L)$_2$(π)]$^+$ (where π = Olefin, Ketone, or Aldehyde; L = PMe$_3$, ᵗBuNC)

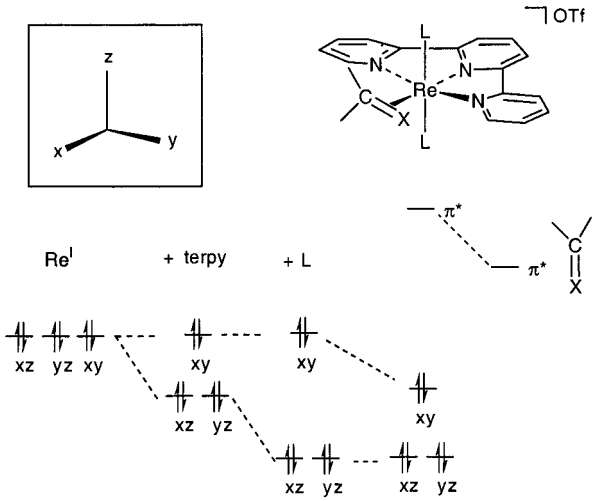

Table 3. Cyclic Voltammogram Data for Selected Complexes

complex	Re(II/I)[a]	Re(I/0)[a]
[Re(terpy)(ᵗBuNC)$_2$(η^2−cyclopentene)][OTf] (**4**)[b]	0.52	−1.38
[Re(terpy)(PMe$_3$)$_2$(η^2−cyclopentene)][OTf] (**5**)[b]	0.22	−1.42
[Re(terpy)(PMe$_3$)$_2$(η^2−benzaldehyde)][OTf] (**7**)[c]	0.28	−1.44
(terpy)Re(Br)(PPh$_3$)(η^2−acetone) (**8**)[c]	−0.04[d]	−1.38
[Re(terpy)(ᵗBuNC)$_2$(η^2−acetone)][OTf] (**9**)[b]	0.46[d]	−1.42
[Re(terpy)(PMe$_3$)$_2$(η^2−acetone)][OTf] (**10**)[c]	0.08[d]	−1.46
[Re(terpy)(ᵗBuNC)$_2$(η^2−acetophenone)][OTf] (**11**)[c]	0.34	−1.32
[Re(terpy)(PMe$_3$)$_2$(η^2−acetophenone)][OTf] (**12**)[c]	0.22[d]	−1.42

[a] Volts vs NHE. [b] In DMA. [c] In acetone. [d] Reported for $E_{p,a}$.

preference for binding in the plane of the terpy ligand. All of the canonical dπ orbitals will be filled in these Re(I) d^6 complexes. If the terpy ligand is assigned to reside in the *xy* plane, both d_{yz} and d_{xz} orbitals will participate in back-bonding with the polypyridyl ligand (Scheme 5). Back-bonding with the isonitrile and phosphine ligands will further stabilize the d_{xz} and d_{yz} orbitals. The HOMO of the {(terpy)Re(L$_2$)}$^+$ fragment would then be the d_{xy} orbital. Thus, binding of π in the *xy* plane would allow maximum dπ metal-to-ligand bonding.

Electrochemistry. Electrochemical experiments provide a convenient analytical technique for characterization of these complexes. Table 3 provides a list of the (II/I) and (I/0) reduction potentials for complexes **4**−**5** and **7**−**12**. The (I/0) reduction potentials are relatively invariant over the series of complexes. Thus, we attribute these couples to ligand-centered (terpy) reductions. Given the poor donating abilities of ketones, the metal-to-ligand π back-bonding interaction is vital to the stability of the η^2-ketone complexes. Therefore, it is not surprising that a single-electron oxidation of the Re^I ketone complexes results in a destabilization of the dihapto-coordinated ketone. In accord with this, the (II/I) oxidation couples for complexes **8**−**10** and **12** are irreversible on the time scale of the cyclic voltammogram experiment (ν = 50−200 mV/s). In contrast to the ketone complexes, the cyclopentene complexes **4** and **5** exhibit reversible (II/I) oxidation waves. The better donating ability of the cyclopentene ligand compared to the ketone ligands and the absence of lone electron pairs capable of η^1 binding likely contribute to the increased

stability of the Re(II) olefin complex compared to its ketone analogues. Interestingly, while the II/I couple for the PMe_3 complex *trans*-[(terpy)$(PMe_3)_2$Re(η^2-acetophenone)][OTf] (**12**) is irreversible, *trans*-[(terpy)-(^{t}BuNC)$_2$Re(η^2-acetophenone)][OTf] (**11**) has a reversible (II/I) oxidation couple. The electron-withdrawing aryl group lowers the energy of the π^* orbital and decreases the d$\pi-\pi^*$ energy gap. As a result, π back-bonding is expected to be more efficient with aryl ketones due to better orbital overlap. It is possible that π back-bonding is operative even for the oxidation product of **11** and that this factor is responsible for an apparent increase in stability compared to acetone. Inconsistent with this hypothesis is the observation that when the ^{t}BuNC ligands are replaced with a weaker π-acid (PMe_3), the II/I oxidation couple becomes irreversible. Apparently, the increased steric bulk of the phosphine ligands relative to isonitrile destabilizes the Re(II) complex of **12**.

The effect of the relative π-acceptor abilities of ^{t}BuNC versus PMe_3 is seen by comparing the (II/I) oxidation potentials for pairs of complexes that differ only in their axial ligands. For example, *trans*-[Re(terpy)(^{t}BuNC)$_2$-(η^2-cyclopentene)][OTf] (**4**) shows a (II/I) reduction potential 300 mV higher than *trans*-[Re(terpy)$(PMe_3)_2$-(η^2-cyclopentene)][OTf] (**5**) (0.52 V versus 0.22 V). This difference in potential is consistent with the greater π-acidity of the isonitrile ligand versus PMe_3. Aldehydes are generally considered to be superior π-acids when compared to ketones (vide supra), and the positive shift for $E_{p,a}$ for the benzaldehyde complex **7** compared to corresponding ketone complexes is consistent with this notion.

Ligand Exchange. As mentioned above, an acetone-d_6 solution of (terpy)(Br)(PPh_3)Re(η^2-acetone) (**8**) undergoes acetone ligand exchange. Partially deuterated acetone (free or bound) was not observed. Thus, ligand exchange is invoked to explain the disappearance of the bound acetone signals rather than proton exchange. In contrast to **8**, even upon heating, the dihapto-acetone complexes **9** and **10** do not undergo analogous exchange reactions. The acetophenone ligand of complexes **11** and **12** is labile, as evidenced by the appearance of free acetophenone and the formation of *trans*-[Re(terpy)$(L)_2$-(η^2-acetone-d_6][OTf] (L = ^{t}BuNC or PMe_3) in an acetone-d_6 solution. In a ^{1}H NMR experiment, treatment of **11** or **12** with cyclopentene yields the corresponding η^2-cyclopentene product. In contrast, the benzaldehyde complexes **6** and **7** show no signs of ligand exchange.

Ligand exchange reactions can in some cases be oxidatively catalyzed. For example, *trans*-[Re(terpy)-(^{t}BuNC)$_2$(η^2-acetone)][OTf] (**9**) shows no signs of exchange in an acetone-d_6 solution after several days at 20 °C. But, addition of a catalytic amount of $[Cp_2Fe][PF_6]$ (Cp = cyclopentadienyl) results in rapid incorporation of acetone-d_6 into the coordination sphere (less than 1 h to >95% completion). This exchange is likely the result of a mechanism similar to that elucidated for the $\{Os(NH_3)_5\}^{2+}$ system.[9h] Here, the catalyst oxidizes the d^6 metal to its d^5 configuration where an η^2 to η^1 linkage isomerization takes place. Once in its η^1 form, rapid ligand exchange may take place. Reversing this sequence of reactions reforms the catalyst.

Scheme 6. Methylation of an η^2-Acetone Ligand by CH_3OTf

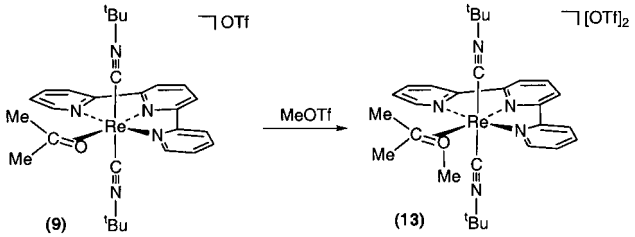

Scheme 7. Resonance Structures for the Methyl Acetonium Complex 13

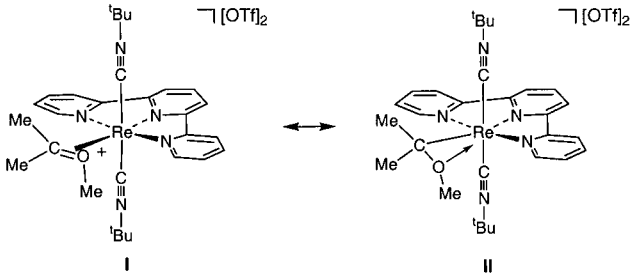

Electrophilic Addition. The electron-rich *trans*-[(terpy)$(L)_2$Re]$^+$ (L = ^{t}BuNC, PMe_3) functions as a potent π base, as evidenced by its ability to bind unsaturated organic molecules in an η^2 fashion. Electron donation from a metal dπ orbital to dihapto-coordinated moieties can serve to activate the η^2 ligands toward electrophilic attack. Reaction of *trans*-[(terpy)(^{t}BuNC)$_2$Re(η^2-acetone)][OTf] (**9**) with MeOTf yields the η^2-ketonium complex *trans*-[(terpy)(^{t}BuNC)$_2$Re{η^2-$(CH_3)_2$C(OMe)}][OTf]$_2$ (**13**) (Scheme 6). A similar methylation has been observed for aldehyde complexes of pentaammineosmium-(II).[15] Complex **13** could be structurally described by several different forms. The actual structure is likely somewhere along the continuum between the two bonding extremes shown in Scheme 7. The methylated acetone ligand in structure **I** remains bound in an η^2 fashion, while structure **II** represents a formal oxidation at the metal center {from Re(I) to Re(III)} and formation of an η^2-methoxymethyl complex. The most compelling evidence that structure **I** dominates is a slight downfield shift for the carbonyl carbon of **13** (92.1 ppm) compared to that of the acetone complex **9** (89.6 ppm). A significant contribution from structure **II** would increase sp^3 character for the carbonyl carbon, resulting in an upfield shift. The methyl group on the oxygen resonates at 4.30 ppm in the ^{1}H NMR spectrum and at 67.9 ppm in the ^{13}C NMR spectrum. The equivalence of the ketone methyl groups and of the ^{t}BuNC ligands in the NMR spectra of **13** suggests that a fluxional process is occurring that is rapid on the time scale of the NMR experiments. Apparently the methyl group on the oxygen undergoes a wiperlike inversion at oxygen that is rapid relative to the NMR time scale.

Conclusions

The complex *trans*-[Re(terpy)$(PPh_3)_2$Br]OTf has proven to be a versatile precursor to the fragments *trans*-

(15) For similar reactions with $[(NH_3)_5Os(\eta^2$-aldehyde$)]^{2+}$ complexes, see: Spera, M. L.; Chen, H.; Moody, M. W.; Hill, M. M.; Harman, W. D. *J. Am. Chem. Soc.* **1997**, *119*, 12772.

$\{(terpy)(L)_2Re\}^+$ (L = ^{t}BuNC or PMe_3). These metal systems show exceptional π-donor ability, as is demonstrated by their propensity toward η^2-coordination of unsaturated organic molecules and by the reactivity of one of these products, *trans*-[Re(terpy)(^{t}BuNC)$_2$(η^2-acetone)]OTf, with methyl triflate.

Experimental Section

General Methods. Unless otherwise noted, all reactions were performed under a dry nitrogen atmosphere in a Vacuum Atmospheres Co. glovebox. ^{1}H and ^{13}C NMR spectra were recorded on a General Electric QE-300 or GN-300 spectrometer at room temperature. All chemical shifts are reported in ppm and are referenced to TMS using residual ^{1}H signals and to the ^{13}C signals of the deuterated solvents. Coupling constants are given in hertz. Electrochemical experiments were performed under a nitrogen atmosphere using a PAR model 362 potentiostat driven by a PAR model 175 universal programmer. Cyclic voltammograms were recorded (Kipp and Zonen BD90 XY recorder) in a standard three-electrode cell from +1.50 to −2.20 V with a glassy carbon working electrode. All potentials are reported vs NHE using ferrocene ($E_{1/2}$ = 0.55 V) or cobaltinium hexafluorophosphate ($E_{1/2}$ = −0.78 V) as internal standard. The peak-to-peak separation ($E_{p,a} - E_{p,c}$) was between 70 and 100 mV for all reversible couples. Elemental analyses were obtained on a Perkin-Elmer PE-2400 Series II CHN analyzer. All distillations were performed under a nitrogen atmosphere. Methylene chloride was distilled from P_2O_5; benzene, hexanes, and diethyl ether were distilled from Na/benzophenone ketyl; methanol was distilled from Mg(OMe)$_2$ (freshly prepared from Mg activated by elemental iodine); acetonitrile and DMA were distilled from CaH_2; and DME was distilled from Na metal. All solvents were thoroughly purged with nitrogen prior to use. Deuterated solvents were deoxygenated by repeated freeze−pump−thaw cycles.

Re(O)(OEt)(Br)$_2$(PPh_3)$_2$ was prepared according to a literature procedure.[16] Magnesium powder (Aldrich, 50 mesh) was activated by treatment with elemental iodine in DME, followed by washing with DMA, acetone, and diethyl ether. All other reagents were used as purchased from commercial sources. Note: Peak assignments for ^{13}C NMR spectra of complexes **6**, **7**, **11**, and **13** were complicated by the large number of resonances in the range of approximately 120−150 ppm. Therefore, isochronous resonances resulted in only partial assignment of these spectra.

Abbreviations: DME = 1,2-dimethoxyethane; DMA = *N*,*N*-dimethylacetamide; NHE = normal hydrogen electrode; TBAH = tetrabutylammonium hexafluorophosphate; terpy = 2, 2′:6′,2″-terpyridine; OTf = trifluoromethanesulfonate (triflate); ^{t}BuNC = *tert*-butylisocyanide.

Re(=N−NC(Ph)O−)(PPh_3)$_2$Br$_2$ (1). This synthesis is a modification of a previously reported procedure.[17] A suspension of Re(O)(OEt)(PPh_3)$_2$Br$_3$ (42.82 g, 45.96 mmol) and excess PPh_3 (43.64 g, 166.00 mmol) in EtOH (2100 mL) was prepared. In a separate flask, $H_2NN(H)C(O)Ph$ (18.62 g, 136.77 mmol) was suspended in EtOH (100 mL). Concentrated HBr (48%, 23.05 g, 136.77 mmol) was slowly added to the EtOH suspension of $H_2NN(H)C(O)Ph$, causing total dissolution. Dropwise addition of the $H_2NN(H)C(O)Ph$/HBr/EtOH solution to the stirring rhenium suspension was made. The reaction solution was refluxed for 1.5 h and then cooled in an ice bath. The precipitate that formed upon cooling was collected by vacuum filtration and was washed with EtOH (2 × 10 mL) and Et_2O (2 × 25 mL). The dark green solid was extracted with hot benzene (∼2 L) and filtered from the remaining orange solid. Solvent removal under reduced pressure yielded a green solid (33.44 g, 73%).

***trans*-[Re(terpy)(Br)(PPh_3)$_2$][OTf] (2).** Complex **1** (10.64 g, 10.60 mmol) was suspended in a benzene/MeOH (1:1 v/v, ∼400 mL) mixture. Terpy (2.671 g, 11.45 mmol) was added to this suspension, and the reaction mixture was refluxed for 3 days. The solution color changed from green to black during the period of reflux. The solution was cooled, and the solvent volume was reduced to 35 mL under vacuum. Filtration yielded a dark black solid. The solid was washed with benzene (3 × 4 mL) and Et_2O (3 × 5 mL) and dried in vacuo. The black solid has been assigned as *trans*-[Re(terpy)(Br)(PPh_3)$_2$][Br] (7.865 g collected, 67%; CV (DMA/TBAH/100 mV/s) $E_{1/2}$ = 0.52 V, $E_{1/2}$ = −0.92 V vs NHE). A portion of *trans*-[Re(terpy)(Br)(PPh_3)$_2$][Br] (3.009 g, 2.72 mmol) was dissolved in MeOH (200 mL). To this solution was added AgOTf (0.701 g, 2.73 mmol) in MeOH (5 mL). A precipitate formed upon addition of the AgOTf. The reaction was stirred for 2 h, and then the solvent volume was brought to approximately 50 mL under reduced pressure. A dark brown precipitate was collected by vacuum filtration and washed with aliquots of MeOH until the washings were brown instead of green. Extraction of the remaining solid with acetone (4 × 100 mL) was performed until an insoluble gray solid remained. The solvent from the extraction was removed under reduced pressure, and the dark brown residue was collected (2.567 g, 82%). CV (DMA/TBAH/100 mV/s): $E_{1/2}$ = 0.52 V, $E_{1/2}$ = −0.94 V vs NHE. Anal. Calcd for $ReC_{52}H_{41}N_3BrF_3O_3P_2S$: C, 53.25; H, 3.52; N, 3.58. Found: C, 53.21; H, 3.83; N, 3.78.

***trans*-[Re(terpy)(^{t}BuNC)$_2$(η^2-cyclopentene)][OTf] (4).** A flask was charged with a DMA suspension of *trans*-[Re(terpy)(PPh_3)$_2$Br]OTf (**2**) (0.100 g) and excess cyclopentene (10 equiv). To the suspension was added excess Mg^0 (1.3 g). The reaction was stirred vigorously for 15 min, and a color change from brown to green was observed. The Mg^0 was filtered off and washed with DME (10 mL). The DME wash was combined with the DMA filtrate. The putative (terpy)Re(Br)(PPh_3)(η^2-cyclopentene) (**3**) can be observed electrochemically ($E_{p,a}$ = 0.1 V) but not isolated. Excess ^{t}BuNC (10 equiv) was added, and the reaction was stirred at room temperature for 30 min followed by heating at 60 °C for 15 min. After cooling to room temperature, the reaction mixture was filtered. The filtrate was slowly added to stirring Et_2O (100 mL), and a precipitate formed. The precipitate was collected by vacuum filtration and washed with Et_2O. The resulting solid was dried in vacuo (44% yield). ^{1}H NMR (acetone-d_6, δ): 9.62 (d, 2H), 8.68 (d, 4H), 7.92 (t, 2H), 7.76 (t, 1H), 7.57 (t, 2H), 4.31 (d, 2H), 3.80 (m, 2H), 2.56 (m, 2H), 1.92 (m, 2H), 0.98 (s, 9H), 0.79 (s, 9H). ^{13}C NMR (acetone-d_6, δ): 157.0 (2C), 154.9 (2CH), 152.6 (2C), 136.3 (2CH), 132.5 (CH), 127.6 (2CH), 123.7 (2CH), 121.3 (2CH), 66.1 (bound cyclopentene, 2CH), 56.7 ({CH_3}$_3$CNC), 56.4 ({CH_3}$_3$-*C*NC), 36.5 (cyclopentene, 2CH_2), 31.6 ({*C*H_3}$_3$CNC), 31.2 ({CH_3}$_3$CNC), 25.2 (cyclopentene, CH_2), bound ^{t}BuNC carbons not well resolved even at large delay times (9s). CV (DMA/TBAH/100 mV/s): $E_{1/2}$ = 0.52 V, $E_{1/2}$ = −1.38 V vs NHE. IR (glaze): ν_{CN} = 2029 cm^{-1}. Anal. Calcd for $ReC_{31}H_{37}N_5F_3O_3S$: C, 46.36; H, 4.65; N, 8.72. Found: C, 45.69; H, 4.80; N, 8.91.

***trans*-[Re(terpy)(PMe_3)$_2$(η^2-cyclopentene)][OTf] (5).** The procedure for complex **4** was followed except PMe_3 was used instead of ^{t}BuNC (66% yield). ^{1}H NMR (acetone-d_6, δ): 9.83 (d, 2H), 8.55 (overlapping d, 4H), 7.70 (t, 2H), 7.39 (m, 3H), 4.63 (m, 2H), 3.89 (m, 2H), 2.77 (m, 2H), 2.03 (m, 1H), 1.98 (m, 1H), 0.24 (dd, 9H, J_{PH} = 1, 8 Hz), 0.12 (dd, 9H, J_{PH} = 1, 8 Hz). ^{13}C NMR (acetone-d_6, δ): 153.8 (2C), 152.9 (2CH), 149.9 (2C), 132.3 (2CH), 127.2 (CH), 126.0 (2CH), 122.1 (2CH), 117.6 (2CH), 65.3 (bound cyclopentene, 2CH), 34.6 (cyclopentene, 2CH_2), 26.1 (cyclopentene, CH_2), 9.7 ({*C*H_3}$_3$P, d, J_{PC} = 26 Hz), 5.7 ({*C*H_3}$_3$P, d, J_{PC} = 26 Hz). CV (DMA/TBAH/100 mV/s): $E_{1/2}$ = 0.22 V, $E_{1/2}$ = −1.42 V vs NHE. Anal. Calcd for $ReC_{27}H_{37}N_3F_3O_3P_2S$: C, 41.11; H, 4.73; N, 5.33. Found: C, 40.43; H, 4.71; N, 4.99.

(16) Chatt, J.; Rowe, G. A. *J. Chem. Soc.* **1962**, 4019.
(17) Chatt, J.; Dilworth, J. R.; Leigh, G. J.; Gupta, V. D. *J. Chem. Soc. (A)* **1971**, 2631.

***trans*-[Re(terpy)(ᵗBuNC)$_2$(η^2-benzaldehyde)][OTf] (6).** Complex **2**, *trans*-[Re(terpy)(Br)(PPh_3)$_2$][OTf] (0.100 g), was suspended in DMA (1 mL) and MeOH (3 mL). Excess benzaldehyde (10 equiv) was added to the suspension, followed by the addition of excess Zn^0/Hg^0 (1.5 g). The reaction was stirred with an observed color change from brown to olive green. After the cyclic voltammagram indicated the disappearance of all of the starting complex (approximately 3 h), the Zn^0/Hg^0 was removed by filtration and washed with MeOH (2 mL). The MeOH washing was combined with the DMA/MeOH filtrate. Excess ᵗBuNC (10 equiv) was added to the filtrate. The reaction was stirred at room temperature for 1 h and then heated overnight at 60 °C. After cooling to room temperature, a precipitate was removed by vacuum filtration and washed with MeOH (3 mL). The combined filtrate was then reduced to an oil. The oil was redissolved in a minimum amount of MeOH (2 mL) and precipitated by slow addition to stirring Et_2O (100 mL). The resulting solid was collected by filtration and dried under vacuum (80% yield). ^{1}H NMR (acetone-d_6, δ): 9.98 (d, 1H), 9.78 (d, 1H), 8.76 (overlapping doublets, 4H), 8.08 (t, 1H), 7.88 (t, 1H), 7.80 (t, 1H), 7.64 (m, 4H), 7.31 (t, 2H), 7.04 (t, 1H), 6.65 (s, 1H), 1.03 (s, 9H), 0.57 (s, 9H). ^{13}C NMR (acetone-d_6, δ): 153.7, 153.4, 153.1, 148.4, 147.7, 147.3, 136.8, 134.1, 130.1, 126.9, 125.5, 125.3, 125.1, 125.0, 122.9, 121.8, 120.3, 119.3 (aromatic C's), 86.1 (bound benzaldehyde, CH), 56.0 ({CH_3}$_3$*C*NC), 55.3 ({CH_3}$_3$*C*NC), 29.9 (CH_3), 29.6 (CH_3), 29.2 (CH_3). The product is > 95% pure by ^{1}H and ^{13}C NMR.

***trans*-[Re(terpy)(PMe_3)$_2$(η^2-benzaldehyde)][OTf] (7).** The procedure for complex **6** was followed (PMe_3 used in place of ᵗBuNC) (93% yield). ^{1}H NMR (acetone-d_6, δ): 10.17 (d, 1H), 9.90 (d, 1H), 8.75 (m, 3H), 8.66 (d, 1H), 7.95 (d, 2H), 7.90 (t, 1H), 7.68 (m, 3H), 7.52 (m, 1H), 7.43 (t, 2H), 7.36 (t, 1H), 6.75 (d, 1H), 0.24 (dd, 9H, J_{PH} = 1, 8 Hz), −0.16 (dd, 9H, J_{PH} = 1, 8 Hz). ^{13}C NMR (acetone-d_6, δ): 152.3 (C), 151.7 (CH), 149.6 (C), 147.5 (C), 147.1 (CH), 146.2 (C), 144.4 (C), 134.9 (CH), 130.5 (CH), 129.0 (CH), 127.6 (CH), 126.0 (CH), 125.6 (CH), 125.5 (CH), 124.3 (CH), 122.8 (CH), 121.2 (CH), 118.8 (CH), 117.0 (CH), 83.6 (bound benzaldehyde, CH), 8.4 ({*C*H_3}$_3$P, d, J_{PC} = 25 Hz), 6.1 ({CH_3}$_3$P, d, J_{PC} = 25 Hz). CV (DMA/TBAH/100 mV/s): $E_{1/2}$ = 0.28 V, $E_{1/2}$ = −1.46 V vs NHE. CV (acetone/TBAH/100 mV/s): $E_{1/2}$ = 0.28 V, $E_{1/2}$ = −1.44 V vs NHE. The product is > 95% pure by ^{1}H and ^{13}C NMR.

***trans*-[Re(terpy)(Br)(PPh_3)(η^2-acetone)] (8).** Excess Mg^0 was added to an acetone (3 mL) suspension of *trans*-[Re(terpy)(PPh_3)$_2$Br][OTf] (**2**) (0.100 g). The reaction mixture was stirred for 1 h, during which time the color changed from brown to green. The Mg^0 was filtered off and washed with acetone (3 mL). The solid was collected upon solvent removal from the filtrate and dried in vacuo (66% yield). ^{1}H NMR (acetone-d_6, δ): 9.82 (d, 1H), 9.48 (d, 1H), 8.58 (d, 1H), 8.28 (d, 1H), 8.12 (d, 1H), 7.71 (d, 1H), 7.39 (m, 2H), 7.29 (t, 1H), 7.18 (m, 6H), 7.11 (m, 1H), 6.95 (m, 6H), 6.62 (t, 1H), 6.55 (m, 3H), 2.61 (s, 3H), 2.41 (s, 3H). CV (acetone/TBAH/100 mV/s): $E_{p,a}$ = −0.04 V, $E_{1/2}$ = −1.38 V vs NHE. The product is > 95% pure by ^{1}H NMR.

***trans*-[Re(terpy)(ᵗBuNC)$_2$(η^2-acetone)][OTf] (9).** The procedure for the preparation of complex **8** was followed. But, rather than isolating **8** after the acetone wash, excess ᵗBuNC was added to the filtrate. The reaction mixture was stirred at room temperature for 1 h, then heated to 60 °C for an additional hour. After cooling to room temperature, the reaction mixture was filtered to remove any precipitate. Addition of the filtrate to stirring Et_2O (10 mL) resulted in precipitate formation. The precipitate was discarded (the first precipitate was mostly the N_2 complex, *trans*-[Re(terpy)(PPh_3)$_2$(N_2)][OTf]. The remaining filtrate was reduced in volume to 2 mL and then precipitated by dropwise addition to Et_2O (75 mL) followed by the slow addition of hexanes (25 mL). The precipitate was collected by vacuum filtration, washed with Et_2O, and dried in vacuo (66% yield). ^{1}H NMR (acetone-d_6, δ): 9.85 (d, 1H), 9.55 (d, 1H), 8.83 (d, 1H), 8.78 (d, 1H), 8.75 (d, 1H), 8.71 (d, 1H), 8.02 (t, 1H), 7.90 (t, 1H), 7.74 (t, 1H), 7.65 (t, 1H), 7.60 (t, 1H), 2.60 (s, 6H), 0.86 (s, 18H). ^{13}C NMR (acetone-d_6, δ): 153.6 (C), 153.3 (C), 152.2 (CH), 148.3 (C), 148.2 (C), 148.1 (CH), 139.4 (d, C, J_{PC} = 13 Hz), 136.4 (CH), 134.1 (CH), 129.2 (CH), 125.8 (CH), 124.7 (CH), 122.9 (CH), 121.4 (CH), 120.3 (CH), 119.2 (CH), 89.6 (bound acetone, C), 55.5 ({CH_3}$_3$*C*NC), 30.2 (CH_3), 29.4 (CH_3). CV (DMA/TBAH/100 mV/s): $E_{p,a}$ = 0.46 V, $E_{1/2}$ = −1.42 V vs NHE. IR (glaze): ν_{CN} = 2083 cm^{-1}. Anal. Calcd for $ReC_{29}H_{35}N_5F_3O_4S$: C, 43.93; H, 4.45; N, 8.83. Found: C, 44.22; H, 4.52; N, 8.68.

***trans*-[Re(terpy)(PMe_3)$_2$(η^2-acetone)][OTf] (10).** The procedure for complex **9** was followed except PMe_3 was used in place of ᵗBuNC (61% yield). ^{1}H NMR (acetone-d_6, δ): 9.98 (d, 1H), 9.59 (d, 1H), 8.74 (overlapping d, 3H), 8.59 (d, 1H), 7.84 (t, 1H), 7.64 (m, 2H), 7.46 (t, 1H), 7.27 (t, 1H), 2.52 (s, 6H), 0.21 (t, 18H, J_{PH} = 3 Hz). ^{13}C NMR (acetone-d_6, δ): 154.3 (C), 152.2 (CH), 151.3 (C), 148.1 (CH and C overlapping), 145.7 (C), 136.3 (CH), 131.6 (CH), 126.3 (CH), 125.4 (CH), 125.1 (CH), 124.3 (CH), 122.0 (CH), 120.3 (CH), 118.4 (CH), 88.7 (bound acetone, C), 33.0 (acetone, CH_3), 9.4 ({CH_3}$_3$P, t, J_{PC} = 2 Hz). CV (DMA/TBAH/100 mV/s): $E_{p,a}$ = 0.12 V, $E_{1/2}$ = −1.44 V vs NHE. CV (acetone/TBAH/100 mV/s): $E_{1/2}$ = 0.08 V, $E_{1/2}$ = −1.46 V vs NHE. Anal. Calcd for $ReC_{25}H_{35}N_3F_3O_4P_2S$: C, 38.56; H, 4.53; N, 5.40. Found: C, 38.65; H, 4.90; N, 5.28.

***trans*-[Re(terpy)(ᵗBuNC)$_2$(η^2-acetophenone)][OTf] (11).** The procedure for complex **6** was followed, except acetophenone was used in place of benzaldehyde (68.0% yield). ^{1}H NMR (acetone-d_6, δ): 10.09 (d, 1H), 9.87 (d, 1H), 8.70 (overlapping d, 4H), 8.06 (t, 2H), 7.84 (m, 2H), 7.70 (d, 2H), 7.68 (t, 1H), 7.30 (m, 2H), 7.03 (t, 1H), 2.80 (s, 3H), 0.94 (s, 9H), 0.50 (s, 9H). ^{13}C NMR (CD_3CN, δ): 153.5 (C), 152.8 (C), 151.9 (CH), 151.5 (C), 148.3 (C), 148.0 (CH), 147.7 (C), 136.6, 134.2, 129.9, 126.8, 125.6, 125.2, 125.0, 124.7, 122.7, 121.4, 120.0, 119.0 (CH), 88.5 (bound acetophenone, C), 55.9 ({CH_3}$_3$*C*NC), 55.1 ({CH_3}$_3$*C*NC), 29.4 (CH_3), 29.0 (CH_3), 28.6 (CH_3). CV (DMA/TBAH/100 mV/s): $E_{p,a}$ = 0.42 V, $E_{1/2}$ = −1.32 V vs NHE. CV (acetone/TBAH/100 mV/s): $E_{1/2}$ = 0.34 V, $E_{1/2}$ = −1.32 V vs NHE. IR (glaze): ν_{CN} = 2083 cm^{-1}. Anal. Calcd for $ReC_{34}H_{37}N_5F_3O_4S$: C, 47.77; H, 4.36; N, 8.19. Found: C, 47.21; H, 4.40; N, 7.61.

***trans*-[Re(terpy)(PMe_3)$_2$(η^2-acetophenone)][OTf] (12).** The procedure for complex **6** was followed (PMe_3 used in place of ᵗBuNC) (46% yield). ^{1}H NMR (acetone-d_6, δ): 10.49 (d, 1H), 9.94 (d, 1H), 8.78 (d, 1H), 8.75 (d, 1H), 8.70 (d, 1H), 8.69 (d, 1H), 7.88 (t, 1H), 7.74 (t, 1H), 7.68 (m, 3H), 7.34 (m, 2H), 7.18 (m, 2H), 6.95 (m, 1H), 2.85 (s, 3H), 0.30 (d, 9H), −0.37 (d, 9H). ^{13}C NMR (acetone-d_6, δ): 153.9, 152.8, 151.9, 149.3, 147.1, 147.0, 144.8, 135.4, 131.7, 130.7, 129.0, 128.1, 127.6, 125.6, 125.3, 124.8, 124.1, 123.0, 120.9, 118.9, 117.0 (aromatic C), 86.8 (bound acetophenone, t, J_{PC} = 4 Hz), 31.6 (acetophenone CH_3), 8.5 ({*C*H_3}$_3$P, d, J_{PC} = 25 Hz), 8.0 ({CH_3}$_3$P, d, J_{PC} = 25 Hz). CV (acetone/TBAH/100 mV/s): $E_{p,a}$ = 0.22 V, $E_{1/2}$ = −1.42 V vs NHE. Anal. Calcd for $ReC_{30}H_{37}N_3F_3O_4P_2S$: C, 42.85; H, 4.44; N, 5.00. Found: C, 42.64; H, 4.37; N, 5.67.

***trans*-[Re(terpy)(ᵗBuNC)$_2$(η^2-acetone(Me))][OTf]$_2$ (13).** 2,6-Di-*tert*-butylpyridine (0.018 g) was added to an acetonitrile solution of *trans*-[(terpy)(tBuNC)$_2$Re(η^2-acetone)][OTf] (**9**) (0.022 g). The solution was cooled to −35 °C, and MeOTf (0.021 g) was added. Upon warming to room temperature, a color change from purple to orange was noted. Slow addition of Et_2O (50 mL) yielded an orange precipitate. The orange solid was collected by vacuum filtration, washed with Et_2O, and dried in vacuo (75% yield). ^{1}H NMR (CD_3CN, δ): 9.18 (d, 1H), 8.76 (d, 1H), 8.65 (d, 1H), 8.61 (d, 1H), 8.54 (d, 1H), 8.51 (d, 1H), 8.08 (t, 1H), 8.00 (t, 1H), 7.97 (t, 1H), 7.76 (m, 2H), 4.30 (s, 3H), 2.60 (s, 6H), 0.90 (s, 18H). ^{13}C NMR (acetone-d_6, δ): 153.3, 150.6, 149.0, 148.8, 139.5 (CH), 138.5 (CH), 137.6 (CH), 127.6 (CH), 127.3 (CH), 124.7 (CH), 124.1 (CH), 121.8 (CH), 92.1 (bound ketonium C), 67.9 (*O*-bound CH_3), 56.8 ({CH_3}$_3$*C*NC), 29.0 (CH_3), 28.9 (CH_3).

Crystal Structure of *trans*-[Re(terpy)(^{t}BuNC)$_2$(η^2-cyclopentene)][OTf]·Et$_2$O (4). A dark purple plate of dimensions 0.38 × 0.32 × 0.11 mm was grown by diffusion of diethyl ether into an acetone solution of **4**. The crystal was determined to be of monoclinic symmetry ($P2_1/n$, No. 14) with the following cell dimensions (λ(Mo) = 0.710 69 Å): a = 14.266(3) Å; b = 15.801(5) Å; c = 17.482(5) Å; β = 107.76(2)°; Z = 4; V = 3758(3) Å^3; F_w = 877.05 ($C_{35}H_{47}N_5O_4F_3SRe$); D_{calc} = 1.55 g/cm^3. Data were collected at −120 °C on a Rigaku AFC6C diffractometer as outlined in Table 1. A total of 5672 data were collected with 5455 unique reflections and 3323 reflections with $I > 3\sigma(I)$. The error fit was 1.79 and final R = 0.047 (R_w = 0.060). Empirical absorption corrections were applied using the ψ scan method with a range of transmission factors of 0.42−1.00.[18]

Crystal Structure of *trans*-[Re(terpy)(^{t}BuNC)$_2$(η^2-acetophenone)][OTf] (11). A black block (0.32 × 0.23 × 0.46 mm) was grown from diethyl ether diffusion into an acetone solution of **11**. The crystal was determined to be triclinic ($P\bar{1}$, No. 2) with the following cell dimensions (λ(Mo) = 0.71069 Å): a = 11.534(5) Å; b = 16.597(7) Å; c = 9.805(4) Å; α = 103.03(3)°; β = 94.90(3)°; γ = 103.13(3)°; Z = 2; V = 1762(3) Å^3; F_w = 854.96 ($C_{34}H_{37}N_5O_4F_3SRe$); D_{calc} = 1.61 g/cm^3. Data were collected on a Rigaku AFC6C diffractometer at −120 °C. A total of 5200 reflections were measured with 4898 unique reflections and 3938 reflections with $I > 3\sigma(I)$. The error fit was 2.27 and final R = 0.056 (R_w = 0.072). Empirical absorption corrections were applied using the ψ scan method with a range of transmission factors of 0.31−1.00.

Acknowledgment is made to the National Science Foundation (NSF Young Investigator Program) and the Alfred P. Sloan Foundation for their generous support of this work.

Supporting Information Available: Tables containing complete positional and thermal parameters, bond lengths, and bond angles for **4** and **11** (19 pages). Ordering information is given on any current masthead page.

OM980500P